Coupling of Spectrin and Polylysine to Phospholipid Monolayers Studied by Specular Reflection of Neutrons

Shirley J. Johnson,* Thomas M. Bayerl,* Wo Weihan,* Heike Noack,* Jeff Penfold,‡ Robert K. Thomas,§ Dawn Kanellas,§ Adrian R. Rennie,‖ and Erich Sackmann*

*Technische Universität München, Physik Department E22, D-8046 Garching bei München, Germany; ‡Rutherford Appleton Laboratory, Chilton Didcot, Oxon OX11 0QX; §Physical Chemistry Laboratory, University of Oxford, South Parks Road, Oxford OX1 3QZ; ‖School of Chemistry, University of Bristol, Cantock's Close, Bristol BS8 1TS, United Kingdom

ABSTRACT The technique of specular reflection of neutrons is applied for the first time to study the charge-dependent interaction of the protein spectrin and the polypeptide poly-L-lysine with model phospholipid monolayers inthe condensed phase state. We first established the structure of a pure monolayer of dimyristolyphosphatidylcholine (DMPC) in both the expanded and condensed fluid phase states without protein in the subphase. The thickness of the hydrocarbon chains increases from 11.4 ± 1.5 Å in the expanded state to 15.8 ± 1.5 Å in the condensed state, whereas the head group region is ~ 10 Å thick for both phase states. When spectrin is present in the subphase, the dimensions of DMPC in the condensed state are not significantly affected, but there is ~ 0.09 volume fraction spectrin in the head group region. Lipid-spectrin coupling is enhanced by electrostatic interaction, as the volume fraction of spectrin in the head group region increases to 0.22 in a mixed monolayer of DMPC and negatively charged dimyristolyphosphatidylglycerol in the condensed state. In contrast to spectrin, polylysine does not penetrate the head group region, but forms a layer electrostatically adsorbed to the charged head groups.

INTRODUCTION

We have recently established that the specular reflection of neutrons is a viable technique for studying phospholipid monolayers at the liquid/air interface (1) and bilayers at the solid/liquid interface (2). One can determine the interfacial structure in substantial detail from reflectivity data, including head group thickness, hydrocarbon chain thickness, and degree of hydration. Here we extend the monolayer studies to consider the coupling of the protein spectrin and the polypeptide poly-L-lysine to lipid monolayers.

Spectrin is the primary element of the membrane-bound cytoskeleton in red blood cells (3–5), and it contributes to structural and viscoelastic properties of the red cell membrane. Spectrin forms an elongated flexible dimer of ~ 1,000-Å contour length, consisting of two intertwined polypeptides with molecular weights of 240,000 and 220,000 D. The association of spectrin with the structural proteins actin, band 4.1, and ankyrin facilitates its binding to intrinsic membrane proteins. It has also been shown, however, that spectrin binds to model phospholipid monolayers even when there are no other proteins present in the system (6–8). In addition, spectrin causes increased permeability of sodium ions (6) and glucose (9) through phospholipid vesicles, providing further evidence for direct spectrin-lipid interaction. Although spectrin has a net negative charge at pH 7, it interacts appreciably with mixtures of dimyristolyphosphatidylcholine (DMPC) and negatively charged dimyristoylphosphatidylserine (DMPS) at pH 7 (6–8, 10).

The interesting interaction of spectrin with phospholipids has prompted varied and sometimes contradictory speculations. Both spectrin and DMPS are located solely on the cytoplasmic side of the erythrocyte membrane, and there is considerable discussion as to whether spectrin plays a role in maintaining phospholipid asymmetry in the membrane (11). Moreover, it is not clear whether spectrin contains specific binding sites for DMPS (10, 12), or if the interaction is electrostatic in nature so that other negatively charged phospholipids produce the same effect. There is also disagreement as to whether hydrophobic forces come into play as well as electrostatic forces in spectrin-lipid interaction (7, 8). The degree of penetration of spectrin into the lipid layer is a further open question. To address some of the above unresolved issues, we investigated the interaction of spectrin with monolayers of pure DMPC and mixed monolayers of DMPC and negatively charged dimyristoylphosphatidylglycerol (DMPG) at the air-water interface.

We also examined the interaction of the polypeptide poly-L-lysine with a mixed monolayer of DMPC/DMPG. Polylysine is positively charged at neutral pH, and so it binds strongly to negatively charged model membranes, (13–15) forming a polypeptide coating at the phospholipid surface without significant penetration into the bilayer. Thus polylysine is a good model for an extrinsic protein, and comparison of the results for polylysine provide insight into spectrin-lipid interaction.

Address correspondence to Dr. Bayerl.

THEORY

The specular reflection of neutrons is rapidly gaining recognition as a powerful technique for elucidating interfacial structure (16, 17). Because of the analogy between reflection of neutrons and of light, one can apply the fundamentals of optics to the phenomenon of specular neutron reflection. For nonadsorbing samples, the neutron refractive index is

$$n = 1 - \lambda^2 Nb/2\pi, \quad (1)$$

where λ is the wavelength of neutrons, N is the atomic number density, and b is the bound coherent scattering length, which is a property of individual atoms. The refractive index profile (or scattering length density profile) normal to an interface can be determined by the specular reflection technique, where reflectivity is measured as a function of momentum transfer normal to the surface, $Q = 4\pi \sin\theta/\lambda$ where θ is the glancing angle as shown in Fig. 1.

Reflectivity data are often analyzed using the optical matrix method (16, 18), where the interfacial structure is divided into a series of flat layers with sharp boundaries. A characteristic matrix can be defined for each layer, and for the jth layer, we have

$$M_j = \begin{vmatrix} \cos\beta_j & -(i/p_j)\sin\beta_j \\ -ip_j \sin\beta_j & \cos\beta_j \end{vmatrix}, \quad (2)$$

where $p_j = n_j \sin\theta_j$ and $\beta_j = (2\pi/\lambda)n_j d_j \sin\theta_j$ where d_j is the thickness of the layer. For n layers, the characteristic matrices are multiplied: $M_R = [M_1][M_2] \ldots [M_n]$. The reflectivity R is calculated from

$$R = \left| \frac{(m_{11} + m_{12}p_s)p_a - (m_{21} + m_{22})p_s}{(m_{11} + m_{12}p_s)p_a + (m_{21} + m_{22})p_s} \right|^2 \quad (3)$$

where m_{ij} designates the elements of the matrix M_R, and subscripts s and a refer to subphase and air, respectively. In applying the optical matrix method, one begins by specifying a model for the interfacial structure, and then proceeds to solve Eq. 3 for reflectivity as a function of momentum transfer Q, adjusting the model as necessary to achieve good fits to the data.

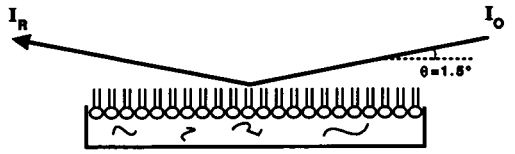

FIGURE 1 Schematic diagram of the experimental arrangement. The lipid monolayer is spread on a subphase containing protein. Incident neutrons of intensity I_0 impinge on the monolayer at glancing angle θ = 1.5°. The neutrons are specularly reflected at the interface and detected as intensity I_R.

MATERIALS AND METHODS

Experimental

We purchased DMPC, DMPC with perdeuterated hydrocarbon chains (DMPC_d_{54}), and DMPG from Avanti Polar Lipids (Birmingham, AL). We synthesized totally deuterated DMPC (DMPC_d_{tot}) according to the method of Kingsley and Feigenson (19). We isolated spectrin according to the method of Gratzer et al. (20, 21). The lyophilized spectrin dimers were stored at −70° and used within several days after preparation. We purchased deuterated water (D_2O) and poly-L-lysine hydrobromide of 289,000 mol wt from Sigma Chemical Co. (Deisenhofen, Germany). Water (H_2O) was ultraclean, purified through an Elga UHQ water purification sysem.

We spread the lipid films on a standard film balance consisting of a 33.5 × 19.5-cm teflon trough equipped with a teflon barrier moved via a stepper motor to effect lateral pressure changes of the monolayer film. We measured the lateral pressure using a Wilhelmy plate device. The entire film balance was enclosed in an air-tight polyethylene box containing mica windows to allow the neutrons to pass through. All measurements were performed at ambient temperature, T ∽ 22°C.

The experiments were conducted using the CRISP spectrometer (22) at Rutherford Appleton Laboratory. CRISP operates at a fixed glancing angle θ = 1.5° as shown in Fig. 1. Specularly reflected neutrons with wavelengths from 0.5 to 6.5 Å are collected on a time of flight basis, and each measurement required from 3–5 h. The minimum reflectivity is determined by the sample dependent background, which arises from incoherent scattering from the aqueous subphase. Detailed procedures have been developed (36) for the reliable subtraction of this background measurements on contrast-matched-air water (for which there is no specular reflection) and show that the incoherent background is uniform over the Q range of these measurements. Furthermore, it is identical to the flat background at high Q for measurements with an adsorbed layer and either background can be used can be used for a reliable background subtraction. Measurements with a multidetector (rather than a single detector) enable the background at each Q value to be determined at "off-specular", and this has been shown to be equivalent to the previous procedures. Finally, it has been shown that there is negligible difference between fitting the data with the background subtracted and including a flat background in model fitting. For convenience the latter procedure is used in this work.

We performed several sets of experiments, each incorporating from two to four different contrasts in scattering length density between subphase and lipid monolayer. Different contrasts are achieved by changing the D_2O content of the subphase and by using selectively deuterated lipids in the monolayer. Pressure-area diagrams were acquired for all phospholipids used in this study with H_2O and D_2O, respectively, as subphase. No significant changes of the pressure-area diagrams were observed due to this isotope substitution of the subphase. The subphase is either pure D_2O or a 91/9 H_2O/D_2O mixture, which has a scattering length density of zero, the same as that of air. We refer to the H_2O/D_2O mixture as contrast-matched-air water (CMA). In the following, DMPC should be taken to signify the DMPC lipid molecule in general, without regards to its degree of deuteration. We used only nondeuterated DMPG, which we denote as simply DMPG. The experiments that we performed include: (*a*) DMPC at lateral pressure $\pi \sim 10$ mN/m: four contrasts including DMPC_d_{tot} on CMA, DMPC_d_{54} on CMA, DMPC_d_{54} on D_2O, and

DMPC_h on D_2O. (*b*) DMPC at $\pi \sim 30$ mN/m: same four contrasts as data set 1. (*c*) DMPC at $\pi \sim 30$ mN/m with spectrin in the subphase: same four contrasts as data set 1. (*d*) 7/3 DMPC/DMPG at $\pi \sim 30$ mN/m: two contrasts including DMPC_d_{54}/DMPG on CMA, and DMPC_d_{54}/DMPG on D_2O. (*e*) 3/2 DMPC/DMPG at $\pi \sim 30$ mN/m with spectrin the subphase: four contrasts including DMPC_d_{tot}/DMPG on CMA, DMPC_d_{54}/DMPG on CMA, DMPC_d_{54}/DMPG on D_2O, and DMPC_h/DMPG on D_2O. (*f*) 3/2 DMPC/DMPG at $\pi \sim 30$ mN/m with polylysine in the subphase: same contrasts as data set 5 excluding DMPC_d_{54}/DMPG on CMA. We also collected reflectivity from subphases containing either spectrin or polylysine without a lipid monolayer, but the results did not differ significantly from those for the pure subphase without protein.

For those experiments with added protein, we buffered the subphase to pH 7 with phosphate buffer (0.03 M Na_2HPO_4/KH_2PO_4 with 10^{-3} M EDTA). In the case of a pure D_2O subphase, we used deuterated buffer, where deuteration of the phosphate salts was accomplished by dissolution in D_2O and repeated evaporation. We added protein to the buffered subphase by injecting a concentrated solution (~ 0.3 mg protein/ml buffered water) under the surface of the subphase with adequate stirring. The final concentration of protein in the subphase was 3.7×10^{-8} M for spectrin and 5.8×10^{-8} M for polylysine. We applied the monolayer film on the protein-containing subphase by spreading a lipid/chloroform solution (1 mg/ml) at the surface. The film was then slowly compressed via the barrier to achieve the desired lateral pressure. Spreading of the film to a low pressure on a subphase containing protein resulted in a gradual increase in surface pressure over several hours. When the film was compressed to a high pressure with polylysine in the subphase, the pressure quickly stabilized after compression. When spectrin was in the subphase, the pressure gradually fell by a few mN/m within approximately an hour to an equilibrium value. We began the measurements after allowing the pressure to stabilize. For samples with protein in the subphase, the pressure fell by at most 3 mN/m during the measurements. Without protein in the subphase, the pressure remained stable within 1 mN/m throughout the measurements.

To check the sensitivity of the lipid monolayer, spectrin interaction to the preparation method (injection of the spectrin into the subphase before or after spreading the lipids) comparative studies on a fluorescence film balance (trough size 10 cm × 2.5 cm) using eosine labeled spectrin were performed. Neither the pressure area diagram nor the fluorescence pattern (and its lateral pressure dependence) were significantly different to the control (speading on the spectrin containing subphase) when the spectrin was carefully injected under the preformed monolayer (3/2 DMPC/DMPG) at low lateral pressure and allowed to equilibrate for 2 h. (Sackmann, E., and T. M. Bayerl, unpublished results).

DATA ANALYSIS

It is important to conduct specular reflection experiments at more than one contrast in scattering length density, as good fits to a single set of reflectivity data can be achieved with a variety of parameter sets (cf reference 23 for a detailed discussion about the use of contrasts). For each layer in the model, there are two parameters to fit: thickness of the layer and its scattering length density. Thus, for a two-layer model, such as we use to describe the lipid, there are four unknown parameters. In our previous preliminary investigations with pure lipid monolayers (1), we used only two contrasts and so were required to make some assumptions to fit the reflectivity data. In the present work, however, reflectivity data for pure lipid without protein requires no assumptions because we studied four contrasts providing ample information to determine the four fitted parameters. Fitting the reflectivity data for lipids with spectrin is less exact, however, because we use a three-layer model containing six parameters.

Fig. 2 shows theoretical scattering-length-density profiles for the four contrasts that we utilized, and these are used as a guide in specifying an appropriate model for the interfacial structure. In reality, the scattering-length-density profile is not a series of sharp steps, but is a continuous function reflecting the scattering lengths of the individual constituent atoms. However, the present resolution of the experiment, determined by Q_{max}, does not warrant a more detailed model of the lipid monolayer than consisting of two distinct layers of uniform scattering length density. In the model fitting, we have constrained the parameters such that this model is self-consistent for all the contrasts. Following the previous arguments (cf theory section) the data has been fitted with a flat background included in the fit.

The first contrast depicted in Fig. 2 represents a

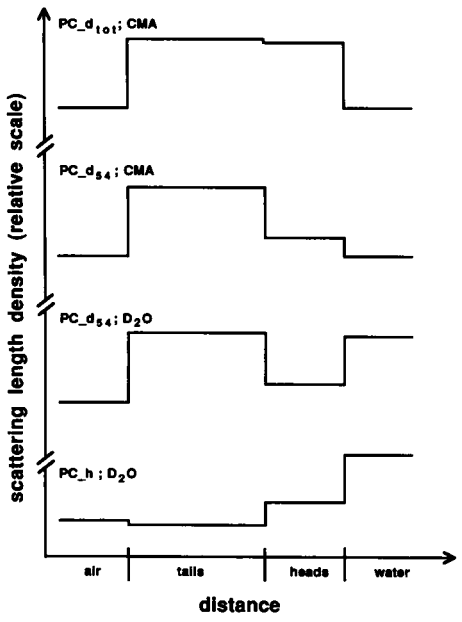

FIGURE 2 Theoretical scattering-length-density profiles for a DMPC monolayer without protein at four different contrasts. The interfaces in the structure are indicated on the abscissa. The degree of lipid deuteration and the subphase are shown for each contrast: PC_d_{tot} is totally deuterated DMPC, PC_d_{54} is deuterated only in the hydrocarbon chains, and PC_h is nondeuterated DMPC. The subphase is either pure D_2O or an H_2O/D_2O mixture contrast matched to air (CMA).

monolayer of DMPC_d_{tot} on a subphase of CMA water. In this case, there is no contribution to reflectivity from the subphase because CMA has the same scattering length density as air, and therefore the measured reflectivity is entirely due to the strongly contrasted lipid monolayer. In the second contrast, where DMPC_d_{54} is used on the same CMA subphase, the tails provide a strong contrast to air, but the scattering length density of the head group is much smaller. The head group is emphasized on the third contrast, however, where the same lipid DMPC_d_{54} is employed, but this time on a subphase of pure D_2O. Finally, in the fourth contrast, the lipid contains no deuterium, so there is little contrast of the tails with air, but there is still a substantial contrast between the heads and the pure D_2O subphase.

The layers in the model are shown schematically in Fig. 3. The first layer of thickness d_1 contains only hydrocarbon tails and air, whereas the second layer d_2 contains head groups, water, and tails. Reflectivity is a time-averaged results, so tail segments can be present in the head group region due to thermal fluctuations. When protein is present in the subphase, there is a third layer d_3 consisting of adsorbed protein and water, and furthermore layer d_2 may also contain protein.

From the fitted scattering length density ρ_j^{fit}, one can calculate the volume fraction of each component in layer j. For layer d_1, we have

$$\rho_1^{fit} = \alpha_{T,1}\rho_T^{theory} + \alpha_{A,1}\rho_A^{theory}, \quad (4)$$

where ρ^{theory} is the theoretical scattering length density of tails (subscript T) and air (subscript A), and $\alpha_{T,1}$ and $\alpha_{A,1}$ are the volume fraction of tails and air, respectively, in layer d_1. Eq. (4) does not introduce any new parameters in our model, because we have the additional equation $\alpha_{T,1} + \alpha_{A,1} = 1$. Thus, we are able to uniquely specify the two quantities $\alpha_{T,1}$ and $\alpha_{A,1}$ with the two equations. For layer d_2, we have

$$\rho_2^{fit} = \alpha_{H,2}\rho_H^{theory} + \alpha_{W,2}\rho_W^{theory} + \alpha_{T,2}\rho_T^{theory} + \alpha_{S,2}\rho_S^{theory}, \quad (5)$$

where subscripts H, T, W, and S refer to heads, tails, water, and spectrin, respectively. Eq. 5 introduces either one new parameter for lipid without protein or two new parameters for lipid with spectrin, but these additional degrees of freedom are eliminated through Eq. 7 below. The components of the adsorbed protein layer d_3 are determined from

$$\rho_3^{fit} = \alpha_{W,3}\rho_W^{theory} + \alpha_{P,3}\rho_P^{theory}, \quad (6)$$

where subscript P indicates protein. Eq. 6 introduces no new parameters, because $\alpha_{W,3} + \alpha_{P,3} = 1$. The theoretical scattering length densities necessary to solve Eq. 4–6 are listed in Table 1. The volumes required to calculate the scattering length densities were taken from references 25 and 37. Note that the proteins have some exchangeable hydrogen atoms, so their scattering length density depends on whether they are dissolved in D_2O or CMA water.

It is possible to measure the area per lipid molecule when the subphase is CMA water. Although both CMA water and air penetrate the lipid monolayer, the scattering length density of both is zero, and so they do not contribute to the fitted scattering length density of the lipid. The area per lipid molecule is

$$\text{area/mol} = \frac{b}{d_1\rho_1 + d_2\rho_2}, \quad (7)$$

where b is the scattering length of the lipid, and d_j and ρ_j are the fitted thickness and scattering length density, respectively, for layer j. Eq. 7 reduces the degrees of freedom in the model by one, because the area per lipid

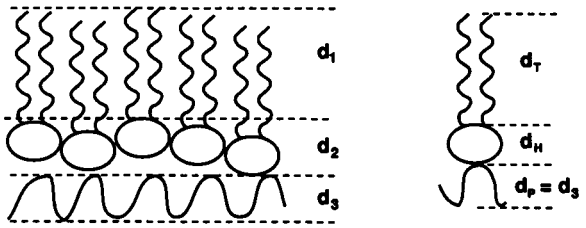

FIGURE 3 Schematic diagram showing the various layers in the model. Layers of thickness d_1, d_2, and d_3 were used in fitting the reflectivity data, where d_1 contains only hydrocarbon tails, d_2 contains heads, water, and tails, and d_3 contains protein and water. For the case of spectrin in the subphase, d_2 also contains spectrin. The thicknesses of the lipid head group and hydrocarbon tails are d_H and d_T, respectively, and are calculated from d_1 and d_2 according to Eq. 8 and 9.

TABLE 1 **Theoretical scattering length densities ($\times 10^{-6}$ Å^{-2}), $T = 22°C$**

Air		0.0
CMA water		0.0
D_2O		6.35
Spectrin (in CMA)		2.03
Spectrin (in D_2O)		2.94
Polylysine (in CMA)		1.27
Polylysine (in D_2O)		2.89
DMPC_h	Head	1.75
	Tail	−0.41
DMPC_d_{54}*	Head	1.75
	Tail	6.65
DMPC_d_{tot}†	Head	6.26
	Tail	6.65
DMPG	Head	2.17
	Tail	−0.41

*Assuming DMPC_d_{54} contains 95% deuterated tails. †Assuming DMPC_d_{tot} contains 95% deuterated tails and 90% deuterated heads.

molecule must be the same for both DMPC_d_{tot} and DMPC_d_{54} on CMA. Furthermore, comparison of area per lipid molecule with and without spectrin permits one to estimate $\alpha_{S,2}$, the volume fraction of spectrin in layer d_2 (see Eq. 5).

The thickness of the lipid hydrocarbon tails d_T is calculated according to

$$d_T = d_1 + (\alpha_{T,2})d_2. \quad (8)$$

Likewise, the head group thickness d_H is

$$d_H = d_2 - (\alpha_{T,2})d_2. \quad (9)$$

The exact value for the volume fraction of tails $\alpha_{T,2}$ in layer d_2 is calculated from Eq. 5, where ρ_2^{fit} represents an average value for the scattering length density across the entire layer d_2. The hydrocarbon tails are, however, confined to the edge of the layer nearest d_1. Thus Eq. 8 and 9 are only approximations for d_H and d_T. We note that $\alpha_{T,2}$ from Eq. 5 is generally on the order of 0.10 corresponding to about one CH_2 group, so d_H and d_T differ from d_2 and d_1, respectively, by only ~ 1 Å.

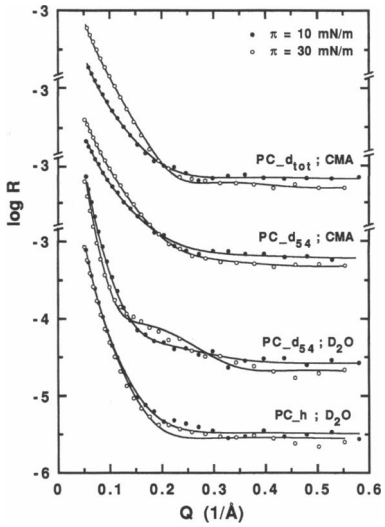

FIGURE 4 Reflectivity as a function of momentum transfer Q for a pure DMPC monolayer (without protein) in the expanded state at π = 10 mN/m (●) and the condensed state at π = 30 mN/m (○), T = 22°C. Four different contrasts are shown, abbreviated the same as in Fig. 2. The solid lines are best fits to the data, from which the values in Table 2 were determined.

RESULTS AND DISCUSSION

Pure lipid monolayer structure

Before examining the coupling of protein to the monolayer, we first established the structure of lipid on a pure aqueous subphase. We measured the reflectivity at two lateral pressures, $\pi \sim 10$ and $\pi \sim 30$ mN/m. At the lower pressure, the lipid is in the expanded state analogous to the liquid-like L_α phase for bilayers. At the higher pressure, the lipid can adopt a condensed liquid crystalline structure.

Fig. 4 shows the reflectivity for DMPC at both the low and high pressures, thus illustrating the difference in reflectivity for the expanded and condensed phase states. In the third contrast (DMPC_d_{54} on D_2O), a slight shoulder is visible in the reflectivity data for high pressure. This can be explained with the help of Fig. 2, where we see that DMPC_d_{54} on D_2O results in three large contrast changes, thus giving rise to interference among the neutrons reflected from the interfaces, and consequently a shoulder in the reflectivity profile appears. This shoulder is not present when the lipid is at low pressure, because there is more air in layer d_1 and also more water in layer d_2. This weakens the features of the scattering length density profile, and the resulting reflectivity curve is smoother when the monolayer is at low pressure. The reflectivity for the fourth contrast (DMPC_h on D_2O) does not differ much between low and high pressure, demonstrating that the primary changes in the monolayer with increasing pressure occur in the hydrocarbon tail region. As shown in Fig. 2, the fourth contrast accentuates the head groups, and so structural changes in the hydrocarbon tails do not greatly affect the reflectivity for the fourth contrast.

Table 2 summarizes the results for the thickness of lipid head group and hydrocarbon tails for DMPC on a pure aqueous subphase. The thickness of the head group shows little change in passing from the expanded state to the condensed fluid state, but the head group dehydrates considerably, in agreement with previous findings (1, 24). The hydrocarbon tails become significantly thicker in the condensed state, and this is expected because compression of the monolayer results in freezing of the hydrocarbon chains into the all-*trans* conformation. The maximum length of a dimyristoyl chain in all-*trans* conformation is 16.7 Å, so we find that the

TABLE 2 **Structure of a DMPC monolayer at lateral pressure π without protein, T = 22°C**

π (mN/m)	d_T (Å)	α_T	α_A	d_H (Å)	α_H	α_W	Area/mol (Å²)
10	11.4	0.70	0.30	9.6	0.30	0.70	87
30	15.8	0.80	0.20	10.7	0.43	0.57	61

Thickness of the tail group is denoted by d_T, and this layer contains volume fractions α_T and α_A of tails and air, respectively. Thickness of the head group is denoted by d_H, and this layer contains volume fractions α_H and α_W of heads and water, respectively. Error in thickness is ±1.5 Å and error in volume fraction is <10% of the listed value.

chains in the condensed state are tilted by an angle of ~19°. The closer packing of the lipid molecules in the condensed fluid state compared with the expanded state is evident from the smaller area per molecule and increased volume fractions α_H and α_T of heads and tails, respectively. Our result for monolayer thickness of 21 Å for DMPC in the expanded state agrees well with results from small-angle scattering studies using vesicles in the L_α phase, where thickness of a monolayer leaflet is reported as 20.5 Å (25), 21..6 Å (26), and 22 Å (27). The small-angle scattering studies do not consider the $L_{\beta'}$ phase, but from x-ray diffraction studies with DMPC lamellae (24, 28), it is reported that a monolayer leaflet in the $L_{\beta'}$ phase is 3.5–4 Å thicker than in the L_α phase. This compares well with our result that DMPC in the condensed state is 4 Å thicker than in the expanded state.

We collected reflectivity data for DMPC_d_{54} on CMA water at several different pressures and calculated the area per molecule as per Eq. 7. Fig. 5 compares the area per molecule determined from reflectivity with that measured on a standard film balance. At low pressure, the results from the two methods agree quite well, but the results diverge with increasing pressure. At higher pressure, the lipid is more densely packed, so there is less air and CMA water in the layer. Thus the calculation is more sensitive to the exact scattering length density of the lipid, and errors such as impurities in the film or incomplete deuteration of the hydrocarbon chains are more evident. Nevertheless, we had expected that the pressure-area data collected from reflectivity measurements should agree more closely with film balance measurements, and we do not yet fully understand the discrepancy.

Effect of spectrin

A comparision of Tables 2 and 3 shows that the presence of spectrin in the subphase does not significantly affect the thickness of either head or tail group regions of DMPC in the condensed state. There is, however, ~0.09 volume fraction spectrin present in the head group region. Accordingly, area per molecule increases by ~10%, and the packing density of the tails decreases by 9% as compared to DMPC without spectrin. A layer of adsorbed spectrin was not found, as the concentration is apparently too low to provide a large enough contrast in scattering length density for detection. The presence of spectrin in the head group region does not necessarily indicate a direct interaction of spectrin with DMPC, as spectrin alone is surface active producing ~14 mN/m surface pressure without any lipid present. Compressing the lipid monolayer to a high pressure, however, forces spectrin back into the subphase. This is evident from the fact that the lateral pressure fell several mN/m after the monolayer was compressed, requiring recompression to achieve the original high pressure. Because high lateral pressure causes spectrin at the surface to return to the subphase, it is possible that spectrin remaining at the surface may be involved in hydrophobic interaction with the lipid. About 20% of the spectrin chain is highly hydrophobic (29), and spectrin is reported to contain a large number of binding sites for hydrocarbon chains (30). Several investigators have proposed that hydrophobic interaction is important in lipid-spectrin coupling (6, 7, 9, 31), although this is still debated (8, 12).

To establish whether electrostatic interaction is important in lipid-spectrin coupling, we examined a binary mixture of DMPC and negatively charged DMPG in the condensed state. In this case, we measure ~0.22 volume fraction spectrin in the head group region of the lipid monolayer, more than twice as much as for pure DMPC. As shown in Table 3, the dimensions of the lipid heads and tails are not significantly affected by the interaction with spectrin compared with DMPC/DMPG without spectrin. The area per molecule increases by ~20%, however, and the volume fraction of tail groups in d_T decreases from 0.86 without spectrin to 0.67 with spectrin. This is consistent with spectrin penetrating the monolayer, forcing the lipid molecules further apart. Adjacent to the lipid head groups is a layer of 5 Å thickness containing 0.10 vol fraction spectrin and 0.90 vol fraction water. This additional layer in the model allows us to better fit the reflectivity data, but it also introduces two additional parameters, i.e., thickness and scattering length density of the layer. The presence of this spectrin/water layer should be taken as a rough representation indicating that the concentration of spectrin diminishes into the subphase. To establish a more accurate picture, additional contrasts would be required preferably using deuterated spectrin, which is not available.

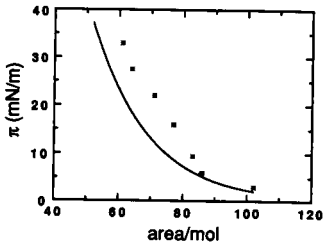

FIGURE 5 Comparison of the pressure-area diagram for a pure DMPC_d_{54} monolayer without protein at T = 22°C as measured on a standard film balance (———) and as determined from reflectivity data (*).

TABLE 3 **Structure of phospholipid monolayers with and without spectrin at π = 30 mN/m, T = 22°C**

Lipid	Spectrin	d_T (Å)	α_T	α_A	d_H (Å)	α_H	α_W	α_S	Area/mol (Å²)	d_S (Å)	α_S	α_W
DMPC	Yes	15.5	0.73	0.27	11.0	0.39	0.52	0.09	68	—	—	—
DMPC/DMPG	No	15.3	0.86	0.14	9.2	0.50	0.50	—	57	—	—	—
DMPC/DMPG	Yes	15.8	0.67	0.33	9.2	0.22	0.56	0.22	81	5	0.10	0.90

For experiments with spectrin, the concentration of spectrin in the subphase was 3.7×10^{-8} M. The hydrocarbon tail region has thickness d_T and contains volume fractions α_T and α_A of tails and water, respectively. The head group has thickness d_H and contains volume fractions α_H, α_W, and α_S of heads, water, and spectrin, respectively. The adsorbed spectrin layer of thickness d_S contains volume fractions α_S and α_W of spectrin and water, respectively. Error in thickness is ±1.5 Å and error in volume fraction is < 10% of the listed value.

Effect of polylysine

The interaction of spectrin with a binary mixture of DMPC/DMPG can be contrasted with the interaction of polylysine with DMPC/DMPG. Polylysine is much less surface active than spectrin, yielding <1 mN/m lateral pressure without lipid present. Consequently, after spreading the monolayer and compressing it to a high pressure, the pressure quickly stabilized without falling as in the case of spectrin indicating that polylysine at the surface readily reenters the subphase. Table 4 shows a comparison of the mixed DMPC/DMPG monolayer structure at high surface pressure with and without polylysine in the subphase. For simplicity, we fit the reflectivity data for pure DMPC/DMPG with a one-layer model consisting of the entire lipid. This results in a slightly smaller total lipid thickness (23 Å compared to 24.5 Å for a two-layer model), because a one-layer model underestimates the contribution of the head groups because the reflectivity is dominated by that of deuterated tail groups, which comprise the majority of the layer. In any case, the contrast in scattering length density between heads and tails is not as pronounced in the mixture since DMPG is nondeuterated, so a one-layer model is appropriate for the mixed monolayer without protein.

To fit the reflectivity profile for DMPC/DMPG with polylysine in the subphase, we used a two-layer model: the first layer for the lipid and the second layer for adsorbed polylysine. Both with and without polylysine, the thickness of the lipid layer is ~23 Å. Polylysine does not penetrate the lipid monolayer itself, but forms a separate layer next to the lipid head groups due to electrostatic attraction, consistent with the results of other investigators (13, 32, 33). The absorbed layer consists of ~0.15 vol fraction polylysine and ~0.85 volume fraction water, indicating that the polylysine is probably loosely packed and does not cover the entire head group surface. Fukushima et al. (34) report that polylysine adopts an ordered structure on binding to DMPC/DMPG vesicles, with both α-helix and β-sheet conformations present. This is strongly dependent on the ratio of lipid to lysine residues, however, with random conformations preferred at lower ratios. In our experiments, the ratio of lipid to lysine residues was on the order of 10^{-3}, so we do not expect that significant ordering of the polylysine occurs. Nevertheless, the adsorbed polylysine seems to affect the lipid packing somewhat, as area per molecule is slightly larger and there is more water in the monolayer. It is expected that polylysine also causes domain formation in mixed lipid membranes (32, 35), but this cannot be directly detected from measurements of reflectivity as a function of Q normal to the surface as we have here.

TABLE 4 **Structure of DMPC/DMPG mixed monolayers with and without polylysine at lateral pressure π = 30 mN/m, T = 22°C**

	d_L (Å)	α_L	α_W	area/mol (Å²)	d_P (Å)	α_P	α_W
Without polylysine	23	0.84	0.16	57	—	—	—
With polylysine	23	0.78	0.22	62	20	0.15	0.85

The entire lipid monlayer has thickness d_L ± 2 Å and contains volume fractions α_L and α_W of lipid and water, respectively. The adsorbed polylysine layer has thickness d_P ± 5 Å, and contains volume fractions α_P and α_W of polylysine and water, respectively. The ratio of DMPC: DMPG is 7:3 without polylysine and 3:2 with polylysine. The polylysine concentration in the subphase was 5.8×10^{-8} M, corresponding to a large excess of lysine residues per lipid molecule.

Alternative model for lipid-spectrin interaction

Given that polylysine is often considered a good model for an extrinsic protein, we applied the model for lipid-polylysine structure to our reflectivity data from the lipid-spectrin system for comparison. As in the case of polylysine, we assume here that spectrin does not penetrate the DMPC/DMPG monolayer, but forms an adsorbed layer next to the head groups. Fig. 6 shows the fits assuming this model, as well as the fits assuming that spectrin does penetrate the head group region. From Fig. 6, one can see that the assumption that spectrin penetrates the head groups has a marked improvement

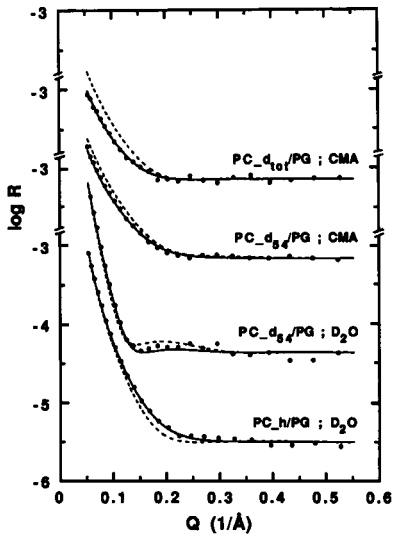

FIGURE 6 Reflectivity as a function of momentum transfer Q for a 3/2 DMPC/DMPG mixed monolayer on a subphase containing 3.7×10^{-8} M spectrin. Four different contrasts are indicated with abbreviations as in Fig. 2. The solid curves are best fits to the data assuming that spectrin penetrates the head group region, and values calculated from the fitted parameters are shown in Table 3. The dashed curves are calculated assuming that spectrin does not penetrate the head group region.

on the quality of the fits. If there were no penetration, the reflectivity data would appear significantly different demonstrating that reflectivity is quite sensitive to the composition of the layers in the model. Fig. 6 illustrates that the alternative model assuming that spectrin couples similar to polylysine is inadequate for fitting the reflectivity data.

CONCLUSIONS

Specular reflection of neutrons reveals that poly-L-lysine and spectrin do not couple in an identical manner with phospholipid monolayers. Polylysine adsorbs electrostatically to mixed monolayers of DMPC/DMPG without penetration into the monolayer. This can be contrasted with spectrin, which penetrates both pure DMPC and mixed DMPC/DMPG monolayers, suggesting that hydrophobic interaction is involved in lipid-spectrin coupling. One might argue that the surface activity of spectrin is at least in part responsible for its presence in the lipid head group region, but nevertheless electrostatic coupling is important in lipid-spectrin interaction as there is significantly more spectrin in the head group region of a charged DMPC/DMPG mixed monolayer compared with an uncharged DMPC monolayer. Spectrin probably adopts a conformation to expose positive charges to the negatively charged DMPG, and this could facilitate the penetration of hydrophobic chain segments into the head group region. The fact that spectrin couples with DMPC/DMPG as well as DMPC/DMPS (6, 7, 8) suggests that the interaction is of an electrostatic nature rather than one involving specificity for serine as is sometimes supposed.

We are indebted to T. Brumm, H. Reinl, and G. Weissmüller for their assistance in performing the experiments. The use of the ISIS facility of the Rutherford-Appleton Laboratory (England) for the experiments is gratefully acknowledged. Dr. Johnson is very grateful to the Alexander von Humboldt-Stiftung for a postdoctoral fellowship.

This research is supported by grants of the Bundesministerium für Forschung und Technologie (No. SA03-TUM), of the Agricultural and Food Research Council (No. FG43/506) and of the Gemeinnützige Hertie-Stiftung (No. GHS 183/89).

Received for publication 8 February 1991 and in final form 10 June 1991.

REFERENCES

1. Bayerl, T. M., R. K. Thomas, J. Penfold, A. Rennie, and E. Sackmann. 1990. Specular reflection of neutrons at phospholipid monolayers: changes of monolayer structure and headgroup hydration at the transition from the expanded to the condensed phase state. *Biophys. J.* 57:1095–1098.
2. Johnson, S. J., T. M. Bayerl, D. C. McDermott, G. W. Adam, A. R. Rennie, R. K. Thomas, and E. Sackmann. 1991. Structure of an adsorbed dimyristoylphosphatidylcholine bilayer measured with specular reflection of neutrons. *Biophys. J.* 59:289–294.
3. Bennett, V. 1985. The membrane skeleton of human erythrocytes and its implications for more complex cells. *Annu. Rev. Biochem.* 54:273–304.
4. Haest, C. W. M. 1982. Interactions between membrane skeleton proteins and the intrinsic domain of the erythrocyte membrane. *Biochim. Biophys. Acta.* 694:331–352.
5. Branton, D., C. M. Cohen, and J. Tyler. 1981. Interaction of cytoskeletal proteins on the human erythrocyte membrane. *Cell.* 24:24–32.
6. Juliano, R. L., H. K. Kimelberg, and D. Papahadjopoulos. 1971. Synergistic effects of a membrane protein (spectrin) and Ca^{2+} on the Na^+ permeability of phospholipid vesicles. *Biochim. Biophys. Acta.* 241:894–905.
7. Mombers, C., J. de Gier, R. A. Demel, and L. L. M. van Deenen. 1980. Spectrin-phospholipid interaction: a monolayer study. *Biochim. Biophys. Acta.* 603:52–62.
8. Maksymiw, R., S.-F. Sui, H. Gaub, and E. Sackmann. 1987. Electrostatic coupling of spectrin dimers to phosphatidylserine containing lipid lamellae. *Biochemistry.* 26:2983–2990.
9. Sweet, C., and J. E. Zull. 1970. Interaction of the erythrocyte-membrane protein, spectrin, with model membrane systems. *Biochem Biophys. Res. Commun.* 41:135–141.
10. Bonnet, D., and E. Begard. 1984. Interaction of anilinonaphtyl labeled spectrin with fatty acids and phospholipids: a fluorescence study. *Biochem. Biophys. Res. Commun.* 120:344–350.

11. Middelkoop, E., B. H. Lubin, E. M. Bevers, J. A. F. Op den Kamp, P. Comfurius, D. T.-Y. Chiu, R. F. A. Zwaal, L. L. M. van Deenen, and B. Roelofsen. 1988. Studies on sickled erythrocytes provide evidence that the asymmetric distribution of phosphatidylserine in the red cell membrane is maintained by both ATP-dependent translocation and interaction with membrane skeletal proteins. *Biochim. Biophys. Acta.* 937:281–288.
12. Bitbol, M., C. Dempsey, A. Watts, and P. F. Devaux. 1989. Weak interaction of spectrin with phosphatidylcholine-phosphatidylserine multilayers: a ^{2}H and ^{31}P NMR study. *FEBS (Fed. Eur. Biochem. Soc.) Lett.* 244:217–222.
13. Hammes, G. G., and S. E. Schullery. 1970. Structure of macromolecular aggregates: II. Construction of model membranes from phospholipids and polypeptides. *Biochemistry.* 13:2555–2563.
14. Carrier, D., and M. Pézolet. 1986. Investigation of polylysine-dipalmitoylphosphatidylglycerol interactions in model membranes. *Biochemistry.* 25:4167–4174.
15. Laroche, G., E. J. Dufourc, M. Pézolet, and J. Dufourq. 1990. Coupled changes between lipid order and polypeptide conformation at the membrane surface: a ^{2}H NMR and Raman study of polylysine-phosphatidic acid systems. *Biochemistry.* 29:6460–6465.
16. Penfold, J., and R. K. Thomas. 1990. The application of the specular reflection of neutrons to the study of surfaces and interfaces. *J. Physics: Condensed Matter.* 2:1369–1412.
17. Russell, T. P. 1991. X-ray and neutron reflectivity for the investigation of polymers. *Material Science Reports 5.* (4, 5) 171–271.
18. Born, M., and E. Wolf. 1959. Principles of Optics. Pergamon Press, London. 803 pp.
19. Kingsley, P. B., and G. W. Feigenson. 1979. The synthesis of a perdeuterated phospholipid: 1,2-Dimyristoyl-sn-glycero-3-phosphocholine-d_{72}. *Chem. Phys. Lipids.* 24:135–147.
20. Ungewickell, E., and W. Gratzer. 1978. Self-association of human spectrin: a thermodynamic and kinetic study. *Eur. J. Biochem.* 88:379–385.
21. Shahbakhti, F., and W. B. Gratzer. 1986. Analysis of the self-association of human red cell spectrin. *Biochemistry.* 25:5969–5975.
22. Penfold, J., R. C. Ward, and W. G. Williams. 1987. A time-of-flight neutron reflectometer for surface and interfacial studies. *J. Phys. E. Sci. Instrum.* 20:1411–1417.
23. Crowley, T. L., E. M. Lee, E. A. Simister, and R. K. Thomas. 1991. The use of contrast variation in the specular reflection of neutrons from interfaces. *Physica B.* In press.
24. Janiak, M. J., D. M. Small, and G. G. Shipley. Temperature and compositional dependence of the structure of hydrated dimyristoyl lecithin. *J. Biol. Chem.* 254:6068–6078.
25. Knoll, W., J. Haas, H. B. Stuhrmann, H.-H. Füldner, H. Vogel, and E. Sackmann. 1981. Small-angle neutron scattering of aqueous dispersions of lipids and lipid mixtures: a contrast variation study. *Appl. Crystallogr.* 14:191–202.
26. Sadler, D. M., E. Rivas, T. Gulik-Krzywicki, and F. Reiss-Husson. 1984. Measurements of membrane thickness by small-angle neutron scattering of suspensions: results for reconstituted rhodopseudomonas sphaeroides reaction-center protein and for lipids. *Biochemistry.* 23:2704–2712.
27. Laggner, P., A. M. Gotto, Jr., and J. D. Morrisett. 1979. Structure of the dimyristoylphosphatidylcholine vesicle and the complex formed by its interaction with apolipoprotein C-III: x-ray small-angle scattering studies. *Biochemistry.* 18:164–171.
28. Janiak, M. J., D. M. Small, and G. G. Shipley. 1976. Nature of the thermal pretransition of synthetic phospholipids: dimyristoyl- and dipalmitoyllecithin. *Biochemistry.* 15:4575–4580.
29. Calvert, R., E. Ungewickell, and W. Gratzer. 1980. A conformational study of human spectrin. *Eur. J. Biochem.* 107:363–367.
30. Isenberg, H., J. G. Kenna, N. M. Green and W. B. Gratzer. 1981. Binding of hydrophobic ligands to spectrin. *FEBS (Fed. Eur. Biochem. Soc.) Lett.* 129:109–112.
31. Sikorski, A. F., K. Michalak, and M. Bobrowska. 1987. Interaction of spectrin with phospholipids: quenching of spectrin intrinsic fluorescence by phospholipid suspensions. *Biochim. Biophys. Acta.* 904:55–60.
32. Hartmann, W., and H.-J. Galla. 1978. Binding of polylysine to charged bilayer membranes: molecular organization of a lipid-peptide complex. *Biochim. Biophys. Acta.* 509:474–490.
33. Papahadjopoulos, D., M. Moscarello, E. H. Eylar, and T. Isac. 1975. Effects of proteins on thermotropic phase transitions of phospholipid membranes. *Biochim. Biophys. Acta.* 401:317–335.
34. Fukushima, K., Y. Muraoka, T. Inoue, and R. Shimozawa. 1989. Conformational study of poly(L-lysine) interacting with acidic phosphlipid vesicles. *Biophys. Chem.* 32:83–90.
35. Mittler-Neher, S., and W. Knoll. 1989. Phase separation in bimolecular mixed lipid membranes induced by polylysine. *Biochem. Biophys. Res. Commun.* 162:124–129.
36. Penfold, J., E. M. Lee, and R. K. Thomas. 1989. The structure of aqueous tetramethylammonium dodecylsulfate solutions at the air-water interface studied by the specular reflection of neutrons. *Mol. Physiol.* 68:33–47.
37. Nagle, J. F., and M. C. Wiener. 1988. Structure of fully hydrated bilayer dispersions. *Biochem. Biophys. Acta.* 942:1–10.